

Lawrence Berkeley National Laboratory

Recent Work

Title

Kinetic Control of Histidine-Tagged Protein Surface Density on Supported Lipid Bilayers

Permalink

<https://escholarship.org/uc/item/4dq2r43p>

Authors

Nye, Jeffrey

Groves, Jay

Publication Date

2008-06-01

Kinetic Control of Histidine-Tagged Protein Surface Density on Supported Lipid Bilayers

*Jeffrey A. Nye¹ and Jay T. Groves^{2,3,4} **

¹Department of Chemical Engineering, and ²Department of Chemistry, University of California, Berkeley, California 94720, and ³Physical Bioscience Division, and ⁴Material Science Division, Lawrence Berkeley National Laboratory, Berkeley, California 94720

* Corresponding author, jtgroves@lbl.gov

RECEIVED DATE:

RUNNING TITLE: Controlling His-Tagged Protein Density on Lipids

ABSTRACT

Nickel-chelating lipids are general tools for anchoring polyhistidine-tagged proteins to supported lipid bilayers (SLBs), but controversy exists over the stability of the protein-lipid attachment. Here, we show that chelator lipids are suitable anchors for building stable, biologically active surfaces, but that a simple Langmuirian model is insufficient to describe their behavior. Desorption kinetics from chelator lipids are governed by the valency of surface binding: monovalently-bound proteins desorb within minutes ($t_{1/2} \sim 6$ min), whereas polyvalently-bound species remain bound for hours ($t_{1/2} \sim 12$ hr). Evolution between surface states is slow, so equilibrium is unlikely to be reached on experimental timescales. However, by tuning incubation conditions the populations of each species can be kinetically controlled,

providing a wide range of protein densities on SLBs with a single concentration of chelator lipid. We propose guidelines for the assembly of SLB surfaces functionalized with specific protein densities, and demonstrate their utility in the formation of hybrid immunological synapses.

INTRODUCTION

As our understanding of biological membranes and membrane-associated proteins grows, new experimental techniques become necessary to probe quantitatively their dynamic role in cellular reaction networks. The silica-supported lipid bilayer (SLB) is an experimental platform uniquely well-suited for these challenges¹. SLBs provide the framework for building well-controlled, biofunctional surfaces while maintaining the hallmark two-dimensional fluidity of cellular membranes. Spatial reorganization of membrane components is emerging as a critical aspect of cell signaling events. Examples include micron-scale pattern formation at cell-cell junctions², pore assembly of antimicrobial peptides³ and oligomerization of neuronal surface receptors⁴. The SLB provides a controllable, mechanically stable substrate for experimentation with such protein networks using optical microscopy and surface sensitive spectroscopies. Recent applications include the use of SLBs to probe protein dynamics during immunological synapse formation^{2,5}, to measure reaction-diffusion kinetics of interferon protein networks^{6,7} and in the controlled display of cadherins for mechanical manipulation⁸.

There are limited chemistries available for incorporating recombinant proteins into SLBs with controlled orientation, while maintaining lateral fluidity. A general solution remains elusive, thus limiting SLBs' experimental flexibility. Nickel-chelating lipids are promising candidates for this task, as they can reversibly tether soluble protein to a fluid lipid layer using histidine tags, an effective and widely-applied affinity handle⁹. However, disparity exists as to the reported nature of the interaction between chelator lipids and histidine-tagged proteins. Several groups have described stable adsorption

of proteins to SLBs containing chelator lipids, and have successfully used such systems for cell-based¹⁰ or electrochemical¹¹ experiments. Others have shown transient surface binding, with rapid desorption of the protein layer^{12,13}, and have sought to counteract these effects by dramatically increasing chelator lipid concentration^{8,14}, lengthening the polyhistidine tail¹⁵, or synthesizing multidentate chelator headgroups^{15,16}. The ease of preparing histidine-tagged proteins^{17,18} make chelator lipids an appealing tool for SLB-functionalization, but a stable surface anchor is necessary for quantitative experimental design. Therefore it is of great interest to understand the reasons for the observed discrepancy.

Here, we systematically study the desorption kinetics of decahistidine-tagged Green Fluorescent Protein (H10-GFP) from SLBs containing nickel-chelating lipids (Ni²⁺-NTA-DOGS), and show that even low concentrations of chelator lipid (1 mol%) are sufficient for building stable protein-functionalized surfaces and that a range of protein surface densities are obtainable with a single concentration of chelator lipid. We show that SLB-bound species exist in multiple association states, from monovalently-bound to polyvalently-bound. Desorption can be described with two steps: a slow transition from poly- to monovalently-bound species, followed by rapid desorption of the monovalently-bound species from the surface. Our results suggest that thermodynamic equilibrium is unlikely to be reached on experimental timescales, so adsorption conditions (incubation time, bulk concentration) can strongly influence the relative populations of poly- and monovalently-bound protein. Thus, SLBs with a single concentration of chelator lipid can be kinetically controlled to exhibit several protein states: stable binding with constant protein density, transient binding in which surfaces undergo rapid protein loss, or a combination of the two. The different unbinding regimes lead to sharply contrasting observations. These findings may account for inconsistencies found in the literature.

We also outline strategies for the preparation of synthetic membrane surfaces with predetermined densities of two different proteins, and show that such surfaces remain functional as artificial antigen

presenting cells for immunological synapse formation with living T-cells.

RESULTS

PREPARING SLBS WITH NICKEL-CHELATING LIPIDS

All experiments were performed with Egg Phosphatidylcholine (EggPC) bilayers containing 1 mol% Ni²⁺-NTA-DOGS (Figure 1, panel b), which displays 14,000 chelator lipids per μm^2 (assuming a lipid cross-sectional area of 72 \AA^2 ¹⁹), which is well below the two-dimensional packing limit of GFP (80,000 and 200,000 proteins per μm^2 , depending on orientation²⁰). Concentrations of up to 10 mol% chelator lipid can be used to form SLBs without noticeable loss of bilayer quality (data not shown). However, Ni²⁺-NTA-DOGS can have undesirable interactions with proteins and other biological molecules, thus a minimum concentration should be used.

HISTIDINE-TAGGED PROTEIN DESORPTION OCCURS IN TWO STEPS

To measure the desorption kinetics of histidine-tagged proteins from nickel-chelating lipids, SLBs were incubated with H10-GFP at 2.5 μM in Tris buffer for 1, 15 and 45 minutes. After washing away unbound protein, surfaces were monitored using fluorescence microscopy under continuous rinsing. Absolute protein densities were calculated by comparing fluorescence intensities to known standards (see Methods), and H10-GFP surface densities were plotted as functions of time (Figure 1).

At short times ($< 1 \text{ hr}$), unbinding traces are well-fit by a single exponential with a vertical offset (Figure 1, panel c), suggesting the presence of two distinct surface species: a transiently-bound species which desorbs with a first-order rate constant of $0.12 \pm 0.02 \text{ min}^{-1}$, and another which remains stable on the surface for at least one hour. Altering the incubation time changes the relative populations of each species, suggesting that protein surface density can be kinetically controlled by altering incubation

parameters. Incubating SLBs with 100 mM EDTA in Tris buffer strips the nickel ion from the chelator lipid, causing complete loss of GFP fluorescence, confirming that both populations are specifically bound through nickel-histidine interactions. Monitoring the H10-GFP surface density of an identically-prepared bilayer for one day shows the slow desorption of the long-lived surface species over the course of hours (Figure 1, panel d). Fitting these data to a biexponential decay gives a desorption rate constant of $9.8 \times 10^{-4} \text{ min}^{-1}$ for the tightly-bound species.

To explain these observations, we propose a quasi-two-step adsorption process (Figure 1, panel a). First, free protein in solution binds to a chelator lipid through a single histidine residue. This monovalently-adsorbed species can then bind additional lipids through other histidines, forming a polyvalent protein-lipid complex, greatly stabilizing the surface species. Bilayer fluidity ensures that even at low chelator lipid densities, each histidine frequently interacts with potential binding sites, and thus the transition from poly- to monovalent binding is slow. After the initial, rapid desorption of monovalently-bound protein, polyvalently-bound protein remains stable on the SLB surface for hours, despite the modest bond energy of a single nickel-histidine interaction. Fluorescence Recovery After Photobleaching (FRAP) experiments with Marina Blue-DHPE tracer lipids showed no significant reduction in bilayer fluidity upon protein adsorption (data not shown).

CONTROLLING SLB PROTEIN DENSITY

The implications of two-state binding on the design of protein-functionalized SLBs were explored experimentally and with quantitative kinetic modeling. Figure 1, panel c indicates that different, stable surface densities of H10-GFP are obtainable on identical SLBs. To fully explore the range of densities achievable with a single chelator lipid concentration, SLBs were incubated with H10-GFP over a wide range of concentrations and times. Bilayers were washed with buffer to remove unbound protein, and surface-bound species were allowed to desorb for one hour before imaging to determine the remaining

density of polyvalently-bound protein (Figure 2, panel a). The results indicate that stable protein density increases monotonically with increasing incubation time and concentration. The rate of increase was dramatically higher for intermediate protein concentrations, and notably, 100-minute incubations at 1.5 μM H10-GFP create SLBs with higher protein densities than incubations at 8.0 μM .

To explain this observation within the context of the two-step adsorption process outlined above, protein binding was modeled using standard first-order kinetic rate equations as follows.

$$\frac{d[\text{AL}]}{dt} = k_1[\text{A}][\text{L}] + k_{-2}[\text{AL}_2] - (k_{-1} + k_2[\text{L}])[\text{AL}]$$

$$\frac{d[\text{AL}_2]}{dt} = k_2[\text{AL}][\text{L}] - k_{-2}[\text{AL}_2]$$

[A] represents bulk protein concentration (assumed to be constant), [L] ligand density, [AL] monovalently-bound protein and [AL₂] polyvalently-bound protein, including all species adsorbed through two or more histidine residues.

Plotting the fractional coverage of polyvalently-bound protein as a function of incubation time for a series of incubation concentrations (Figure 2, panel b) reveals qualitative agreement with the data in Figure 2, panel a: protein surface density increases with increasing incubation time and concentration. However, high protein concentrations quickly saturate surface binding sites, preventing subsequent binding of additional lipids and the formation of multidentate complexes. Incubating at intermediate protein concentrations bypasses this kinetic trap, allowing for the transition to polyvalently-bound surface species, creating bilayers with higher stable protein densities. Surface reorganization continues between 10 and 100 minute incubations for all protein concentrations, indicating that thermodynamic equilibrium is unlikely to be achieved under most experimental conditions. A consequence of this non-

equilibrium behavior is that despite rapid saturation of binding sites, long incubations are necessary to achieve surfaces with stable protein densities. Moreover, the density of polyvalently-bound protein can be maximized by incubating at intermediate protein concentrations; increasing protein concentration in the bulk does not necessarily increase protein density on the surface.

This observed cross-over in protein density is more pronounced if the model explicitly includes higher-order complexes (proteins bound through three histidines, four histidines, etc.) using developed models for polyvalent binding²¹. All ten histidine residues are capable of interacting with chelator lipids, though they may be sterically hindered from doing so, both by packing constraints from other adsorbed proteins, and by conformational constraints within the polyhistidine tag itself. The actual molecule likely exists as an ensemble of many bound states; however the simplification of combining all higher-order complexes into one species sufficiently recapitulates the observed phenomena, and is useful in guiding experimental design.

DESIGNING SYNTHETIC MEMBRANE SYSTEMS: THE HYBRID T-CELL SYNAPSE

A well-established application of protein-functionalized SLBs is in the formation of hybrid immunological synapses, in which live T-cells interface with synthetic membrane surfaces displaying adhesion and signaling molecules from an Antigen Presenting Cell (APC)^{2,5}. Such SLBs require that multiple proteins be tethered to the model APC surface for 60 minutes or more at 37°C, so a strong surface attachment is necessary. To demonstrate the utility of the nickel-histidine anchoring system, we engineered SLBs simultaneously displaying two histidine-tagged protein variants: major histocompatibility complex (MHC) and intercellular adhesion molecule 1 (ICAM) through chelator lipids. The two-state binding model predicts that surfaces with a specific protein density can be prepared in several ways: incubating SLBs at high protein concentrations for short periods of time, or low protein concentrations for long periods of time. SLBs with identical densities of a decahistidine-

tagged fusion of ICAM and the yellow fluorescent protein (ICAM-YFP-H10) were prepared via two methods. SLBs containing 1 mol% Ni²⁺-NTA-DOGS were incubated with ICAM-YFP-H10 for 10 minutes at 100 nM or for 100 minutes at 20 nM in Tris buffer. Excess protein was washed away and surface densities were monitored with fluorescence microscopy (Figure 3). The two sets of incubation conditions lead to similar protein surface densities, but one SLB required five times more protein to prepare.

SLBs functionalized through chelator lipids are biologically active and can serve as model APC membranes, as illustrated by the formation of hybrid immune synapses. SLBs displaying histidine-tagged MHC and ICAM-YFP-H10 activate T-cells and trigger the formation of mature immunological synapses (Figure 4), in which surface proteins form patterns of concentric rings across the T-cell surface. ICAM and its ligand, leukocyte function associated protein 1 (LFA), form an outer ring several microns in diameter, while MHC and its ligand, T-cell receptor (TCR) migrate towards the center. T-cell activation was also confirmed by monitoring intracellular calcium flux with fura-2 (data not shown).

DISCUSSION

Nickel-chelating lipids are promising anchors for the attachment of proteins to synthetic lipid membranes with controlled orientation, while maintaining two-dimensional fluidity. The interaction provides a framework by which many histidine-tagged proteins can be bound in parallel to SLBs, opening a wealth of experimental possibilities for studying surface-based reaction networks. Controversy exists, however, regarding the reversible nature of the interaction. Several groups have reported significant rates of desorption of histidine-tagged proteins from surfaces decorated with chelator lipids, with measured K_D values in the 0.1 – 1 μ M range^{15,22,23}, which would preclude their use

in most quantitative experiments. Conversely, others have used such surfaces for a variety of applications without addressing desorption^{8,10,11}, implying that surface density remains constant over the experimental timecourse. Growing interest in membrane-mediated biochemical systems, and the potential of nickel-chelating lipids as a general tool for attaching proteins to SLBs makes this an important disparity. How can an adsorption reaction with a micromolar K_D be a suitable anchor for SLB-based experiments?

Here, we show that simple, Langmuirian binding is insufficient to explain the interaction between histidine-tagged proteins and SLBs containing chelator lipids. Adsorption can be adequately described by an idealized two-step binding model, although a higher degree of multivalent binding may occur. Initially, free protein in solution binds to a chelator lipid through a single histidine residue. Due to fluidity of the bilayer, this monovalently-bound species can then bind additional lipids through other histidines, forming a tightly-bound protein-lipid complex. This reorganization of surface species is slow compared to incubation times commonly used in the laboratory, which are often less than 10 min^{16,24}. Previous analyses have assumed thermodynamic equilibrium of surface-bound species, and although the chelator lipid binding sites are quickly saturated by monovalently-bound protein, our results suggest that true equilibrium occurs on the timescale of hours to days. Thus over experimentally-relevant timescales, the slow evolution to and from multivalent states must be taken into consideration to fully understand the kinetic behavior of these systems.

The quasi-two-state binding model supports the argument that chelator lipids are suitable anchors for the functionalization of SLBs with histidine-tagged proteins, but with the important caveat that surfaces must be allowed to shed the bulk of the monovalently-bound protein before experimentation begins. At room temperature, this desorption occurs from bilayers containing 1 mol% Ni²⁺-NTA-DOGS with a half-time of 6 ± 1 min. After the period of initial unbinding is complete – 10 to 20 minutes – surface

densities remain essentially constant for several hours, due to the slow transition from poly- to monovalent binding. We believe this phenomenon to be the source of confusion in previously reported desorption rates: surfaces exhibit rapid desorption at short times, especially after short incubations (less than 10 minutes) of high protein concentrations (greater than 10 μM). Fitting this desorption to a Langmuirian binding model indeed gives a high K_D , however this fails to account for the more stably-bound polyvalent fraction, which has significantly slower desorption.

An equally important observation is that by altering incubation conditions, (time and concentration), SLBs with a single concentration of chelator lipid can be tuned to display specific amounts of polyvalently-bound protein. Thus, a variety of experimental conditions can be obtained with a single lipid stock. Likewise, there are multiple avenues to a given protein density. Short incubations at high concentrations lead to surfaces primarily decorated with monovalently-bound species, most of which desorb within minutes. Long incubations at low protein concentrations create the opposite scenario, in which adsorbed species are primarily polyvalently-bound, and show little desorption over hours. Both strategies can be controlled to display identical protein densities at long times, however one uses protein far more efficiently.

Surfaces functionalized with two proteins simultaneously retain biological activity, which we demonstrate with the formation of a hybrid immunological synapse. Live T-cells interface with SLBs decorated with histidine-tagged MHC and ICAM proteins, forming the canonical “bulls-eye” protein pattern.

The immunological synapse is just one of many intercellular junctions experimentally accessible with SLB systems. As our understanding of these and other membrane-based reaction networks grows, so will our need to experiment with more complex, densely-populated synthetic membrane surfaces. The

interaction between nickel-chelating lipids and histidine-tagged proteins is a promising strategy for the parallel incorporation of entire protein reaction networks in a fluid, well-controlled manner. We believe the insights into the kinetic nature of this binding strategy presented here will aid in the design of such surfaces.

METHODS

BILAYER PREPARATION

EggPC bilayers containing 1 mol% Ni²⁺-NTA-DOGS (Avanti) and 4 mol% Marina Blue-DHPE (Invitrogen) were prepared by standard methods. Lipids were mixed in chloroform and dried under vacuum for several hours. Lipid films were resuspended in deionized water to 2 mg/mL and extruded through 100 nm pore filters (Whatman) ten times to create small unilamellar vesicles (SUVs). SLBs were formed over either silica coverslips cleaned in Piranha solution (1:4 mixture of 30% H₂O₂ and sulfuric acid) or 6M NaOH-cleaned glass-bottomed 96-well plates (Nalg Nunc International). SUVs were incubated in 10 mM Tris and 153 mM NaCl buffer for 30 minutes before washing away unfused vesicles with 5 mL Tris buffer.

PROTEIN PREPARATION

Green Fluorescent Protein with a decahistidine tag at its N-terminus (H10-GFP) was expressed in *E. coli*²⁵. Twelve hours after inducing expression with 1 mM IPTG, cells were harvested and lysed, and H10-GFP recovered on a Sepharose-Ni²⁺-NTA affinity column. Protein was eluted with an imidazole gradient and stored in Tris buffer with 10% glycerol. Secreted ICAM-YFP fusion protein with a decahistidine tag at its C-terminus was expressed in HEK-293T cells grown in DMEM media via transient transfection with Lipofectamine 2000 (Invitrogen). Three days after transfection, protein was recovered on an Agarose-Ni²⁺-NTA affinity column (Invitrogen). Similarly, lines of S2 cells expressing

MHC Class II I-E^K with hexahistidine tags on the C-terminus of both alpha and beta chains (a gift of L. Teyton and M. Davis) were grown in Excell 420 media^{26,27}. Protein expression was induced with the addition of 250 mM CuSO₄, and after two days the secreted protein was recovered on an Agarose-Ni²⁺-NTA affinity column. Both MHC and ICAM-YFP-H10 were eluted with an imidazole gradient and stored in Tris buffer with 10% glycerol.

DESORPTION EXPERIMENTS

SLBs were formed in Biopetechs flowcells or glass-bottomed 96-well plates, loaded with 100 mM NiCl₂ in Tris buffer for 5 minutes, and incubated with protein, washing with 5 mL of Tris buffer between each step. Unbound protein was rinsed away with an additional 5 mL of buffer and imaged via epifluorescence with a 0.6 NA 40x objective on a Nikon TE-300 microscope. Exponential fits were performed using OriginPro 7.

Protein densities were measured by comparing GFP and YFP fluorescence intensities to bilayers containing known amounts of the fluorescent lipid BODIPY-FL-DHPE (Invitrogen). To account for spectral differences between the fluorophores, solutions of H10-GFP, ICAM-YFP-H10 and BODIPY-FL-DHPE were prepared with identical fluorophore concentrations and imaged on the microscope and in a Varian Cary Eclipse fluorimeter. The ratio of the solutions' fluorescences was used to map BODIPY-FL-DHPE surface concentration to that of GFP and YFP (manuscript in preparation).

BINDING MODEL

Numerical modeling was performed using Matlab version 7.1. Species surface densities were calculated using the *ode45* algorithm for ordinary differential equations.

IMMUNOLOGICAL SYNAPSES

Artificial APC-cell surfaces were prepared essentially as described² with the following modification: GPI-linked MHC and ICAM were replaced with histidine-tagged variants. MHC was loaded with 50 μ M MCC antigenic peptide overnight at 37°C in pH 4.5 citrate buffer. SLBs were then incubated with both proteins at 200 nM for 100 minutes in HEPES buffer. Flowcells were warmed to 37°C and rinsed with 10 mL buffer. Live murine AND CD4⁺ T-cells were injected 20 minutes later. The T-cell surface protein, TCR, was labeled with F_{AB} fragments of the non-blocking H57 antibody labeled with Alexa568 dye (Invitrogen). Images were acquired 10 to 30 minutes after T-cells contact with the bilayer using a 1.3 NA 100x oil-immersion objective on a Nikon TE-300 microscope.

ACKNOWLEDGEMENTS

This work was supported by the Director, Office of Science, Office of Basic Energy Sciences, of the U.S. Department of Energy under Contract DE-AC03-76SF00098. Molecular graphics images were produced using the UCSF Chimera package from the Resource for Biocomputing, Visualization, and Informatics at the University of California, San Francisco (supported by NIH P41 RR-01081).

This manuscript has been authored by an author at Lawrence Berkeley National Laboratory under Contract No. DE-AC02-05CH11231 with the U.S. Department of Energy. The U.S. Government retains, and the publisher, by accepting the article for publication, acknowledges, that the U.S. Government retains a non-exclusive, paid-up, irrevocable, world-wide license to publish or reproduce the published form of this manuscript, or allow others to do so, for U.S. Government purposes.

FIGURE CAPTIONS

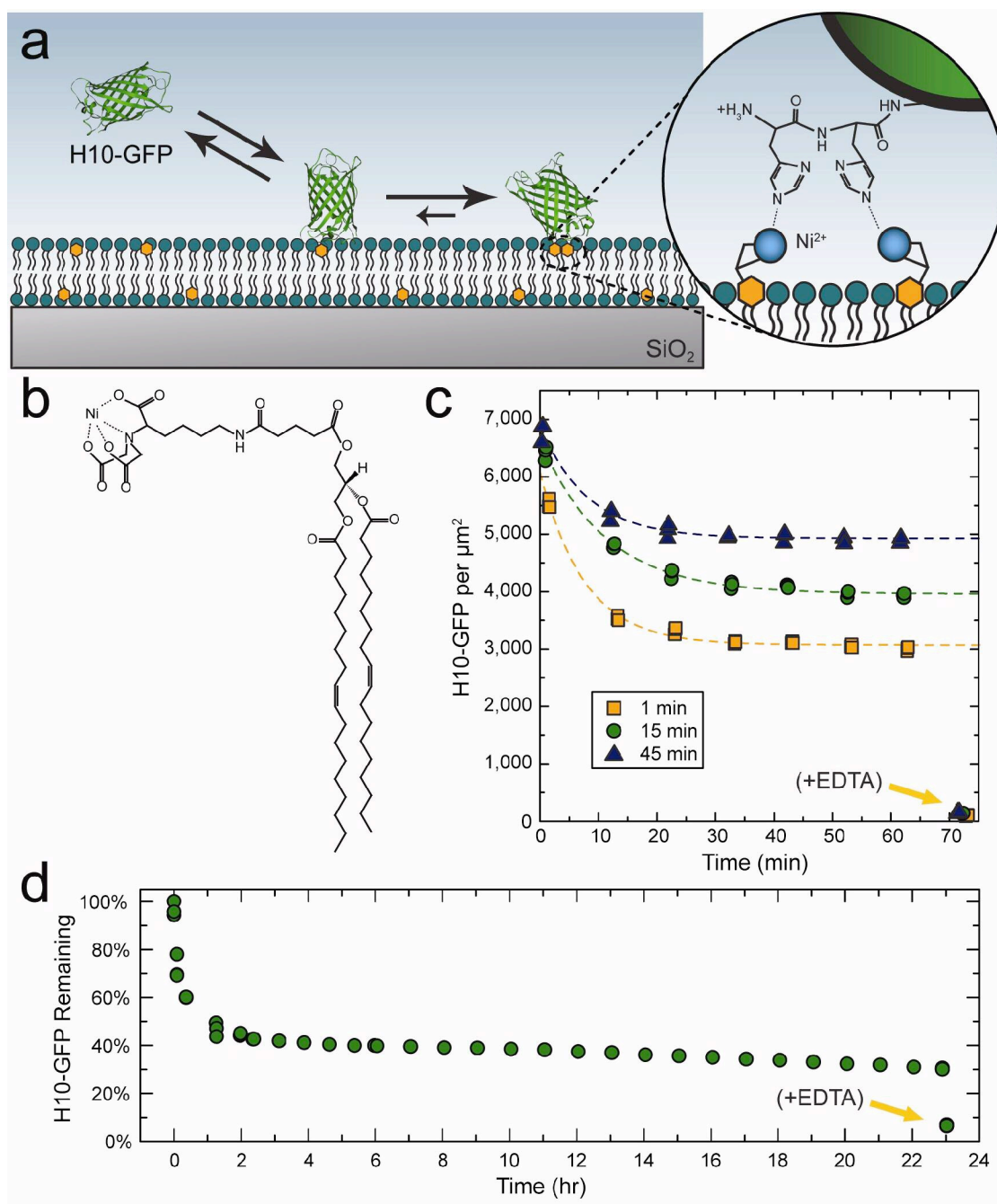


Figure 1. H10-GFP unbinding from supported lipid bilayers containing 1 mol% Ni²⁺-NTA-DOGS, monitored by fluorescent microscopy. a) Schematic illustrating the proposed two-state binding model. Histidine-tagged proteins initially bind to a single lipid. Due to lateral diffusion of the chelator lipids, additional nickel-histidine interactions may accumulate, forming long-lived multidentate protein-lipid complexes. b) Chemical structure of the chelator lipid, Ni²⁺-NTA-DOGS. c) H10-GFP unbinding after

incubations at 2.5 μM for 1, 15 and 45 minutes. Data are fit to a single exponential with a vertical offset, ($k_{-1} \sim 0.12 \text{ min}^{-1}$). d) H10-GFP unbinding after 2.5 μM incubation for 15 minutes showing slow desorption over 23 hours ($k_{-2} \sim 9.8 \times 10^{-4} \text{ min}^{-1}$). Yellow arrows (c, d) indicate data points taken after washing with 100 mM EDTA for 5 minutes to measure nonspecific binding. These points were not included in exponential fits.

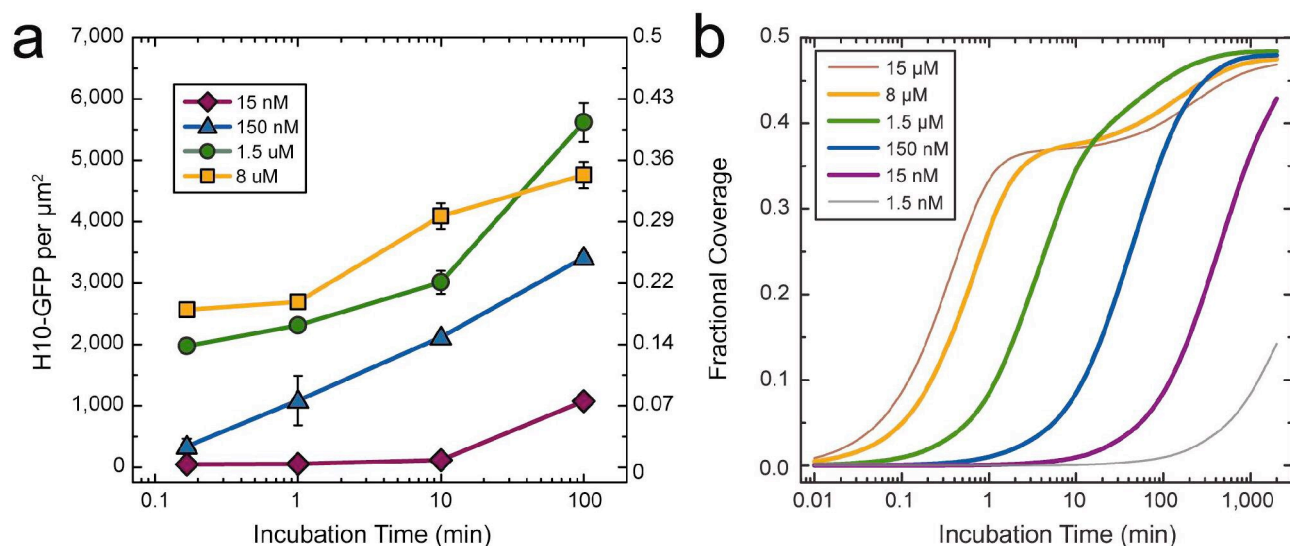


Figure 2. H10-GFP surface density as a function of incubation conditions. a) H10-GFP surface coverage after 60 minutes of unbinding from bilayers containing 1 mol% Ni^{2+} -NTA-DOGS as a function of incubation time and concentration, plotted in protein per μm^2 (left axis) and fractional coverage (proteins per nickel-chelating lipid, right axis). Incubations at high protein concentrations quickly saturate surface binding sites, preventing the formation of polyvalent complexes. Intermediate concentrations allow this transition to proceed, thus achieving higher surface densities during long incubations. b) Numerical solutions to the proposed rate equations show qualitative agreement: coverage of polyvalently-bound protein is maximized at intermediate incubation times and concentrations.

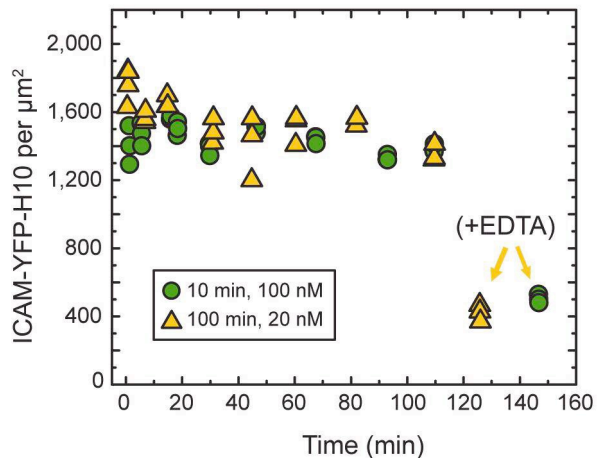


Figure 3. ICAM-YFP-H10 surface density as a function of time on supported lipid bilayers containing 1 mol% Ni^{2+} -NTA-DOGS. Surfaces with similar protein densities can be created with different bulk protein concentrations by varying incubation time. Yellow arrow indicates data points taken after washing with 100 mM EDTA for 5 minutes to measure nonspecific binding.

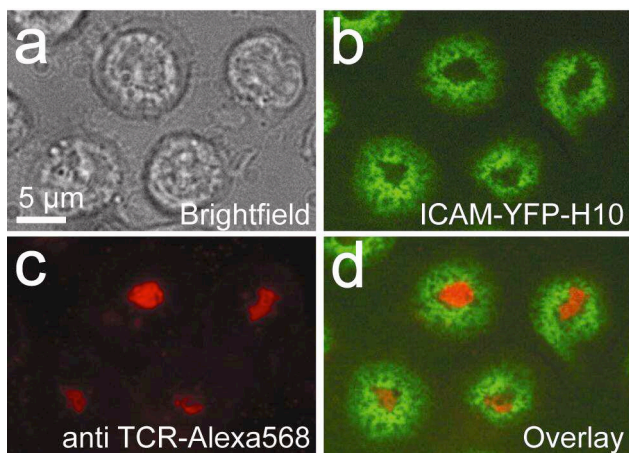


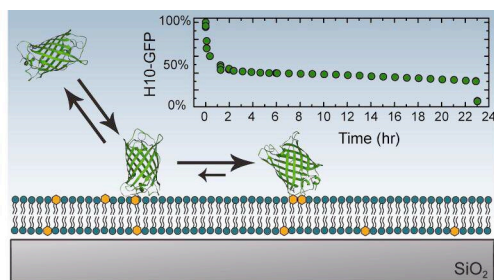
Figure 4. T-cell synapses on supported bilayers containing 1 mol% Ni^{2+} -NTA-DOGS functionalized with histidine-tagged ICAM and MHC, imaged by fluorescence microscopy. Images taken after 10 minutes of incubation at 37°C . a) Brightfield. b) ICAM-YFP-H10. c) anti-TCR-Alexa568. d) Overlay of ICAM-YFP-H10 (b) and anti-TCR-Alexa568 (c).

REFERENCES

- (1) Sackmann, E. *Science* **1996**, *271*, 43-48.
- (2) Grakoui, A.; Bromley, S. K.; Sumen, C.; Davis, M. M.; Shaw, A. S.; Allen, P. M.; Dustin, M. L. *Science* **1999**, *285*, 221-227.
- (3) Brogden, K. A. *Nat Rev Microbiol* **2005**, *3*, 238-250.
- (4) Dean, C.; Scholl, F. G.; Choih, J.; DeMaria, S.; Berger, J.; Isacoff, E.; Scheiffele, P. *Nat Neurosci* **2003**, *6*, 708-716.
- (5) Mossman, K. D.; Campi, G.; Groves, J. T.; Dustin, M. L. *Science* **2005**, *310*, 1191-1193.
- (6) Lamken, P.; Lata, S.; Gavutis, M.; Piehler, J. *J Mol Biol* **2004**, *341*, 303-318.
- (7) Gavutis, M.; Lata, S.; Lamken, P.; Muller, P.; Piehler, J. *Biophys J* **2005**, *88*, 4289-4302.
- (8) Sivasankar, S.; Briehner, W.; Lavrik, N.; Gumbiner, B.; Leckband, D. *P Natl Acad Sci USA* **1999**, *96*, 11820-11824.
- (9) Kubalek, E. W.; Legrice, S. F. J.; Brown, P. O. *J Struct Biol* **1994**, *113*, 117-123.
- (10) Krogsgaard, M.; Li, Q. J.; Sumen, C.; Huppa, J. B.; Huse, M.; Davis, M. M. *Nature* **2005**, *434*, 238-243.
- (11) Tanaka, M.; Hermann, J.; Haase, I.; Fischer, M.; Boxer, S. G. *Langmuir* **2007**, *23*, 5638-5644.
- (12) Sigal, G. B.; Bamdad, C.; Barberis, A.; Strominger, J.; Whitesides, G. M. *Anal Chem* **1996**, *68*, 490-497.
- (13) Dorn, I. T.; Eschrich, R.; Seemuller, E.; Guckenberger, R.; Tampe, R. *J Mol Biol* **1999**, *288*, 1027-1036.
- (14) Somersalo, K.; Anikeeva, N.; Sims, T. N.; Thomas, V. K.; Strong, R. K.; Spies, T.; Lebedeva, T.; Sykulev, Y.; Dustin, M. L. *J Clin Invest* **2004**, *113*, 49-57.
- (15) Lata, S.; Piehler, J. *Anal Chem* **2005**, *77*, 1096-1105.
- (16) Lata, S.; Gavutis, M.; Piehler, J. *J Am Chem Soc* **2006**, *128*, 6-7.

- (17) Hochuli, E.; Bannwarth, W.; Dobeli, H.; Gentz, R.; Stuber, D. *Bio-Technol* **1988**, *6*, 1321-1325.
- (18) Hochuli, E.; Dobeli, H.; Schacher, A. *J Chromatogr* **1987**, *411*, 177-184.
- (19) Vacklin, H. P.; Tiberg, F.; Thomas, R. K. *Bba-Biomembranes* **2005**, *1668*, 17-24.
- (20) Yang, F.; Moss, L. G.; Phillips, G. N. *Nat Biotechnol* **1996**, *14*, 1246-1251.
- (21) Lauer, S.; Goldstein, B.; Nolan, R. L.; Nolan, J. P. *Biochemistry-Us* **2002**, *41*, 1742-1751.
- (22) Dorn, I. T.; Neumaier, K. R.; Tampe, R. *J Am Chem Soc* **1998**, *120*, 2753-2763.
- (23) Dorn, I. T.; Pawlitschko, K.; Pettinger, S. C.; Tampe, R. *Biol Chem* **1998**, *379*, 1151-1159.
- (24) Gizeli, E.; Glad, J. *Anal Chem* **2004**, *76*, 3995-4001.
- (25) Whitehead, T. A.; Boonyaratanakornkit, B. B.; Hollrigl, V.; Clark, D. S. *Protein Sci* **2007**, *16*, 626-634.
- (26) Malherbe, L.; Hausl, C.; Teyton, L.; McHeyzer-Williams, M. G. *Immunity* **2004**, *21*, 669-679.
- (27) Sumen, C.; Dustin, M. L.; Davis, M. M. *J Cell Biol* **2004**, *166*, 579-590.

SYNOPSIS TOC



“Kinetic Control of Histidine-Tagged Protein Surface Density on Supported Lipid Bilayers”

Jeffrey A. Nye and Jay T. Groves

For Table of Contents Use Only

DISCLAIMER

This document was prepared as an account of work sponsored by the United States Government. While this document is believed to contain correct information, neither the United States Government nor any agency thereof, nor the Regents of the University of California, nor any of their employees, makes any warranty, express or implied, or assumes any legal responsibility for the accuracy, completeness, or usefulness of any information, apparatus, product, or process disclosed, or represents that its use would not infringe privately owned rights. Reference herein to any specific commercial product, process, or service by its trade name, trademark, manufacturer, or otherwise, does not necessarily constitute or imply its endorsement, recommendation, or favoring by the United States Government or any agency thereof, or the Regents of the University of California. The views and opinions of authors expressed herein do not necessarily state or reflect those of the United States Government or any agency thereof or the Regents of the University of California.